Rakytska et al. Nanoscale Research Letters (2015) 10:472
DOI 10.1186/s11671-015-1179-6

Nanoscale Research Letters
a SpringerOpen Journal

NANO EXPRESS Open Access

Manganese(II) Complexes with Schiff Bases Immobilized on Nanosilica as Catalysts of the Reaction of Ozone Decomposition

Tetyana Rakytska[1*], Alla Truba[1], Evgen Radchenko[2] and Alexander Golub[2,3]

Abstract

In this article, we submit the description of synthesis and identification of manganese(II) complexes with pyrogenic nanosilica-immobilized ($d_{av} = 10$ nm; $S_{sp} = 290$ m^2/g) hydroxyaldimine ligands $\left(Mn(L)_2/\bar{S}i\right)$: salicilaldiminopropyl (L1); 5-bromosalicilaldiminopropyl (L2); 2-hydroxynaphtaldiminopropyl (L3); 2-hydroxy-3-methoxybenzaldiminopropyl (L4); 2-hydroxy-3,5-dichloroacetophenoniminopropyl (L5); and 4-hydroxy-3-methoxybenzaldiminopropyl (L6). The ligands and complexes were characterized by UV-VIS and IR spectrometry. Nanocomposites consisting of complexes $Mn(L)_2/\bar{S}i$ showed a high catalytic activity in low-temperature ozone decomposition in the range of concentrations between 2.1×10^{-6} and 8.4×10^{-6} mol/l. The number of catalytic cycles increased for isostructural pseudotetrahedral complexes $Mn(L)_2/\bar{S}i$ (L1–L5) in the following order: $Mn(L3)_2 >> Mn(L4)_2 > Mn(L1)_2 > Mn(L2)_2 > Mn(L5)_2$. In the case of pseudooctahedral complexes with L6, the change of coordination polyhedral does not influence the kinetics and stoichiometric parameters of the reaction.

Keywords: Nanosilica, Manganese(II) complexes, Schiff bases, Catalytic ozone decomposition

Background

Dissolved complexes of 3d metals with Schiff bases, especially Mn(II, III) and Co(II) complexes, are used successfully as catalysts of many oxidation reactions of organic compounds [1]. Manganese-Schiff base complexes like square planar Mn(salen) (where salen is *N,N′*-bis(salicilald)ethylenediiminato(2-)anion) have shown considerable promise in superoxide dismutase (SOD) and catalase-like activity which could be a perspective for the creation of new medicines with wide applications [2]. However, difficulties of complex dimerization and extraction of the product and catalyst from solution, as well as the endeavor of modeling natural enzymatic systems, stimulated the research of synthesis of immobilized homogeneous catalysts of oxidation including complexes with Schiff bases [3]. At the beginning, synthetic polymeric materials based on styrene were widely used as carriers of the complexes [4–8]. There are efforts to use, instead of synthetic polymers, natural polymers as carriers for Schiff base complexes with, for example, chitosan that is easily degraded and well combined with human blood, which makes them promising in biomedical practice [9, 10]. Although anchored complexes demonstrated positive properties compared with homogeneous analogs (the raise in catalytic activity and the number of catalytic cycles, selectivity) [6, 7], however, they had lower stability after increasing the temperature of the reaction. Due to this, other avail-

* Correspondence: tlr@onu.edu.ua
[1]Odesa I.I. Mechnikov National University, 2 Dvoryanska str., Odesa 65082, Ukraine
Full list of author information is available at the end of the article

able carriers characterized by chemical, thermal, and mechanical stability can be widely applied. As such carriers, different forms of activated carbon [11–14], dispersed silica of various origins [15–18], zeolites [19–23], and ordered mesoporous molecular sieves, for example, MCM-41 and MCM-48 [24], can be used.

These carriers are characterized by a high internal surface; therefore, immobilization of complexes takes place on both the outer and inner surfaces. In the latter case, an access of reagents to the immobilized complexes and, consequently, the kinetics of the reaction are determined by internal diffusion factors. Intradiffusious inhibition of the reaction with metal-Schiff base complexes can be avoided if non-porous pyrogenic nanosilica (aerosil) with developed outer surface is used as a carrier [25]. It should be noted that manganese(II) becomes manganese(III, IV) in the course of the synthesis of immobilized complexes with Schiff bases on the noted carriers, except nanosilica [25] and aminated silica [17].

Analysis of data obtained as a result of the study of catalytic properties of 3d metal complexes with Schiff bases in the oxidation of organic compounds [15, 17, 18, 20–22, 24, 26–28] and decomposition of ozone [29, 30] leads to the conclusion that the catalytic activity of the immobilized metal complexes in redox reactions can be controlled by the following: (i) optimization of the structural characteristics of the carrier and the method of synthesis for obtaining the homogeneous structure and composition of immobilized complexes, (ii) changes in the geometric configuration of an immobilized complex, and (iii) redistribution of the electron density at the central atom and the ligand leading to a significant change in redox potential of M^{n+1}/M^{n+} pair and, hence, to the reactivity and catalytic activity of the complexes.

All the abovementioned aspects of the synthesis and catalytic activity of nanosilica-immobilized manganese(II)-Schiff base complexes in the reaction of ozone decomposition have not been studied.

The aim of this work is to study the influence of the nature of pyrogenic nanosilica-immobilized Schiff bases on the structure and catalytic activity of manganese(II) complexes in the reaction of ozone decomposition.

Methods

Pyrogenic nanosilica (model A-300, d_{av} = 10 nm, S_{sp} = 290 m^2/g) was purchased from VAT Oriana (Kalush, Ukraine) and was used for synthesis of γ-aminopro pylsilica (APS) (the concentration of aminopropyl groups, $[H_2NC_3H_6–]$, is 0.7 mmol/g SiO_2) by routine procedure [31, 32] used for the synthesis of ligands. Immobilized Schiff bases (L1–L6) salicilaldiminopropyl (L1); 5-bromosalicilaldiminopropyl (L2); 2-hydrox ynaphtaldiminopropyl (L3); 2-hydroxy-3-methoxybenzaldiminopropyl (L4); 2-hydroxy-3,5-dichloroacetoph enoniminopropyl (L5); and 4-hydroxy-3-methoxybenzaldiminopropyl (L6) were obtained from APS by known methods by the following scheme [31].

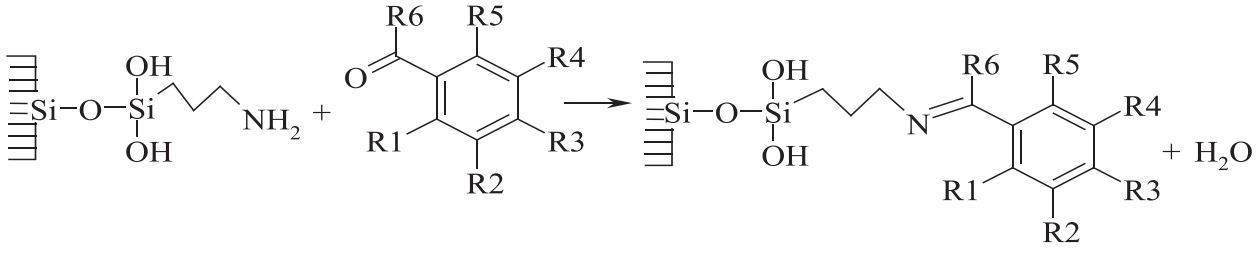

L1 = R1 – OH; R2, R3, R4, R5, R6 – H;

L2 = R1 – OH; R2, R3, R4, R6– H; R5 – Br;

L3 = R1 – OH; R2, R5, R6 – H; R3+R4 – (-CH=CH-CH=CH-);

L4 = R1 – OH; R2 – OCH_3; R3, R4, R5, R6 – H;

L5 = R1 – OH; R2, R4 – Cl; R3, R5 – H, R6 – CH_3;

L6 = R1, R4, R5, R6 – H; R2 – OCH_3; R3 – OH.

Complexes $Mn(L)_2/\bar{S}i$ (L = L1–L6) were obtained by sorption on modified nanosilica from the absolute alcohol solution of dehydrated $MnCl_2$; the concentration before sorption was 10^{-2} mol/l, and Mn^{2+}(solution): L(surface) ratio was 1:2. Concentrations of the immobilized ligands and chemical compositions of the obtained complexes are shown in Table 1.

IR spectra were recorded by a Fourier transform Perkin Elmer Spectrum BX FT-IR instrument (400–4000 cm^{-1}) from transparent tablets obtained by the pressing of bare samples and the addition of KBr as well.

Diffuse reflectance spectra were recorded at room temperature in the wave number range of 30,000–11,000 cm^{-1} by a Specord M-40 in stainless steel cells where the samples were pressed in.

The catalyst samples (m = 0.2 g) were tested using a gas flow setup with a fixed-bed reactor at 20 °C, relative humidity of 65 %, and ozone-air mixture (OAM) linear velocity of 6.2 cm/s. Ozone decomposition was monitored by measuring the final ozone concentration $\left(C^{\mathrm{f}}_{\mathrm{O_3}}\right)$. The initial ozone concentrations $\left(C^{\mathrm{in}}_{\mathrm{O_3}}\right)$ and $C^{\mathrm{f}}_{\mathrm{O_3}}$ were measured either by a Tsyclon-Reverse optical gas analyzer (detection limit of 1 mg/m^3).

The reaction rate (W) was calculated based on the data of ozone concentration change after passing the OAM through the static bed of the catalyst using the following equation:

$$W = \frac{\omega\left(C^{\mathrm{in}}_{\mathrm{O_3}} - C^{\mathrm{f}}_{\mathrm{O_3}}\right)}{m_{\mathrm{cat}}}, \mathrm{mol/(g{\cdot}s)}, \quad (1)$$

where $\omega = 1.67 \times 10^{-2}$ is the OAM volume flow rate, l/s; $C^{in}_{O_3}$ and $C^{f}_{O_3}$ are the initial and final ozone concentrations, respectively, in the OAM, mol/l; and m_{cat} is the weight of a catalyst sample, g.

The initial reaction rate, W_{in}, was defined as W after 1 min of experiment.

The kinetic constants (k_1) at the beginning of the experiment (after 5–10 min) and at 50 % conversion of ozone ($k_{1/2}$) were found from the first-order rate equations:

$$k_1 = \frac{1}{\tau} \ln \frac{C^{\mathrm{in}}_{\mathrm{O_3}}}{C^{\mathrm{f}}_{\mathrm{O_3}}}, \mathrm{s^{-1}}, \quad (2)$$

$$k_{1/2} = \frac{0.69}{\tau_{1/2}}, \ \mathrm{s^{-1}}. \quad (3)$$

where $\tau_{1/2}$ is the ozone half-conversion time.

The amount of ozone that entered the reaction over the course of the experiment (Q_{exp}, moles of O_3) was calculated as the area under the corresponding ozonogram plotted as a $\Delta C_{\mathrm{O_3}}$ vs. τ function. This magnitude was used for the calculation of the following stoichiometric coefficients: $n_{\mathrm{L}} = Q_{\mathrm{exp}}/Q_{\mathrm{L}}$ characterizing the number of moles of ozone per mole of an immobilized ligand (Q_{L}); $n_{\mathrm{Mn}} = Q_{\mathrm{exp}}/Q_{\mathrm{Mn}}$ giving the number of moles of ozone per mole of manganese(II) in the complex; and $n_{\mathrm{CH}} = Q_{\mathrm{exp}}/Q_{\mathrm{CH}}$ showing the extent of mineralization of the hydrocarbon part of a ligand (Q_{CH} is the number of moles of ozone required for complete oxidation of the hydrocarbon part of a molecule calculated relying on the stoichiometry of reactions (4)–(8)).

$$\mathrm{L1/\bar{S}i} \quad 3C_7H_6 + 17O_3 = 21CO_2 + 9H_2O \quad (4)$$

$$\mathrm{L2/\bar{S}i} \quad 6C_7H_5 + 33O_3 = 42CO_2 + 15H_2O \quad (5)$$

$$\mathrm{L3/\bar{S}i} \quad 3C_{11}H_8 + 26O_3 = 33CO_2 + 12H_2O \quad (6)$$

$$\mathrm{L4/\bar{S}i \ and \ L6/\bar{S}i} \quad 3C_8H_8 + 20O_3 = 24CO_2 + 12H_2O \quad (7)$$

$$\mathrm{L5/\bar{S}i} \quad 3C_8H_6 + 19O_3 = 24CO_2 + 9H_2O. \quad (8)$$

Table 1 Complexes of Mn(II) with Schiff bases immobilized on nanosilica

Sample	$C_L \times 10^4$, mol/g	Concentration of Mn(II)	
		$C_{Mn2+} \times 10^4$, mol/g	C_{Mn2+}, wt%
$Mn(L1)_2$	7.0	0.60	0.30
$Mn(L2)_2$	7.0	0.80	0.44
$Mn(L3)_2$	7.0	0.17	0.09
$Mn(L4)_2$	7.0	0.80	0.46
$Mn(L5)_2$	5.0	1.60	0.66
$Mn(L6)_2$	7.0	0.70	0.38

Results

Composition and Structure of Mn(II) Complexes

The spectral characteristics of Schiff bases immobilized on nanosilica, $L/\bar{S}i$ (L = L1–L6), and their complexes with manganese(II), $Mn(L)_2/\bar{S}i$, are summarized in Table 2. In the IR spectra of all complexes except $Mn(L5)_2/\bar{S}i$ was observed a low-frequency shift of a peak (5–15 cm^{-1}) characterizing stretching vibrations of the imino group (C=N) compared with free ligands that indicates an electron density transfer in Mn–N=C bond. Furthermore, in the $Mn(L4)_2/\bar{S}i$ complex, alongside with a low-frequency shift of a $\nu_{C=N}$ band at 1650 cm^{-1}, a peak with lower energy appears at 1620 cm^{-1} which can indicate the finding of ligand L4 in two different configurations. In the case of ligand L6 characterized by two absorption peaks at 1650 and 1600 cm^{-1}, a complex formation results in the high-frequency shift of the first of them whereas the second one remains without alteration.

Table 2 Spectral characteristics of nanosilica-immobilized Schiff bases and $Mn(L)_2/\bar{S}i$ complexes

Ligand complex	Wave numbers of peak maximums, cm^{-1}	
	$\nu_{C=N}$	$\nu_{\pi-\pi^*}$
L1	1635	24,600
$Mn(L1)_2/\bar{S}i$	1630	24,900
L2	1642	29,700; 23,900; 19,400
$Mn(L2)_2/\bar{S}i$	1630	29,800; 24,000; 19,600
L3	1640	23,600; 25,400
$Mn(L3)_2/\bar{S}i$	1630	23,600; 25,400
L4	1650	23,600
$Mn(L4)_2/\bar{S}i$	1645; 1620	24,800; 25,000
L5	1650	23,960
$Mn(L5)_2/\bar{S}i$	1630	24,300
L6	1650; 1600	25,000
$Mn(L6)_2/\bar{S}i$	1665; 1600	27,200; 25,600

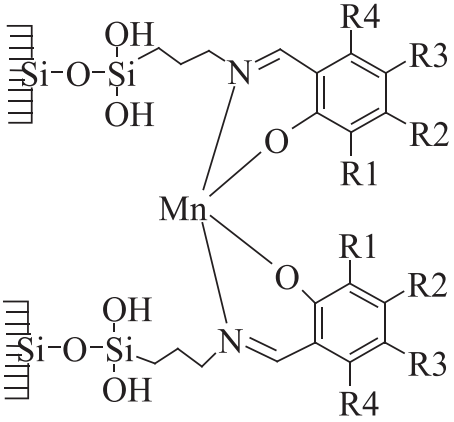

Scheme 1 Structure of the manganese(II) complexes with ligands L1-L5

In UV-VIS spectra after complexation, the high-frequency shift occurs for the peaks characterizing the electron density transfer in ligand $\nu_{\pi-\pi^*}$, compared with a free immobilized Schiff base. Furthermore, in some cases, additional bands appear. Similar changes were observed in the spectra of complexes $Co(L)_2/\bar{S}i$ and $Cu(L)_2/\bar{S}i$ (L = L1–L6) [29, 30].

Sometimes, oxidation of manganese(II) to manganese(III) was observed, which was evidenced by the appearance of an asymmetrical low-intensity shoulder in the visible part of spectrum at 18,500 cm^{-1} (510 nm) that can be relied to a d-d electron transfer in complexes of the square-pyramidal geometry [33–35].

The results of our research have shown that in the visible part of spectrum for all synthesized Mn(II) complexes, a d-d electron transfer is not detected which can be one of the proofs of a stable oxidation state of the complexing ion. A similar example is the synthesis of Mn(II)(salen) complexes on porous amino silica gel (Si-NH_2) [17]. A comparison of the spectral data for similar Cu(II) and Co(II) [29, 30] complexes and $Mn(L)_2/\bar{S}i$ complexes permits to conclude that, for manganese(II), polyhedron N_2O_2 also realizes in the ligand field of L1–L5 (Scheme 1).

Compared with a square planar structure for individual crystalline Schiff base complexes, complexes immobilized on a silica surface suffer a tetrahedral distortion due to the anchoring of a ligand foot to the nanoparticle surface, and that can be one of the causes of a raise in their reaction activity. The tetrahedral distortion of immobilized bis-ligand complexes (except the pseudo octahedral complex with L6) is confirmed by modeling the surface clusters by molecular-mechanical methods (MM2) and by semi-empirical quantum chemistry methods (PM3) as well.

L6, unlike the isomeric L4, cannot form chelate cycles, and coordination with the Mn(II) ion is carried out only by an azomethine group (Scheme 2), which leads to the high-frequency shift of the peak assigned to C=N group vibrations and the ligand charge transfer ($\pi-\pi^*$).

Thus, all synthesized $Mn(L)_2/\bar{S}i$ complexes differ by both the nature of the Schiff base immobilized on nanosilica and the structure of a coordination polyhedron. It is of interest to test the influence of the distinctive factors on the activity of manganese(II) complexes in the reaction of ozone decomposition.

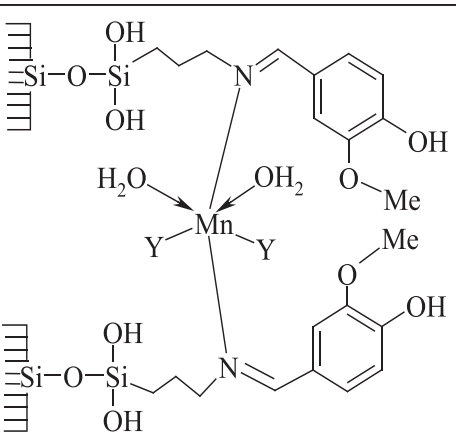

Scheme 2 Structure of the manganese(II) complex with ligands L6

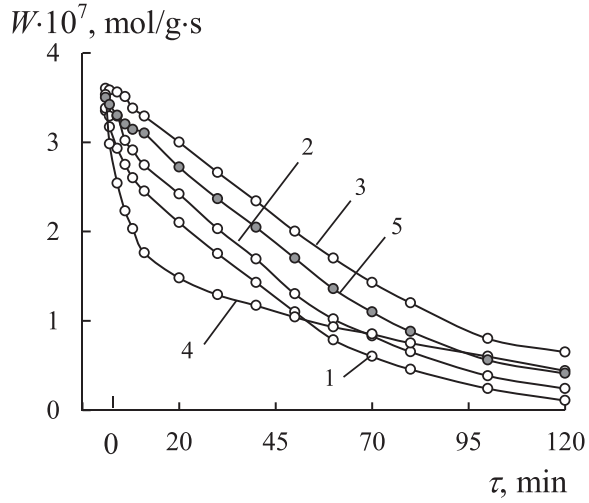

Fig. 1 The time dependence of W for ozone decomposition by L/$\bar{S}$i ligands: L1 (*1*); L3 (*2*); L4 (*3*); L5 (*4*); L6 (*5*) $\left(C^{in}_{O_3} = 4.2 \times 10^{-6}\text{mol/l}\right)$

Testing L/$\bar{S}$i Nanocompositions in the Reaction of Ozone Decomposition

Ozone can interact practically with all organic compounds at low temperature. Hence, at the beginning, the kinetics of ozone decomposition by nanosilica-immobilized Schiff bases, L/$\bar{S}$i (L = L1–L6), would be studied. Time (τ) dependences of the reaction rate (W) for ozone decomposition by the nanocompositions under study (Fig. 1) show that, regardless of the ligand nature, the type of kinetic curves is the same, i.e., the reaction rate decreases in time. In the case of L5 (curve 4), the reaction rate for the first 20 min decreases more drastically. The results of the kinetic and stoichiometric analysis of the obtained data will be discussed hereafter.

Testing $Mn(L2)_2/\bar{S}i$ Nanocompositions in the Reaction of Ozone Decomposition

Time dependences of the reaction rate in the case of ozone decomposition by $Mn(L2)_2/\bar{S}i$ complexes (L = L1–L6) are presented in Fig. 2. It can be seen that the duration of runs varies from 50 min for the L1 ligand up to 1000 min for the L4 ligand (that run was interrupted before the final reaction rate drop). A portion of the kinetic curves for the first 100 min (Fig. 2b) allows to make the differences between the activities of the manganese(II) complexes more clear. The data of Fig. 2b show that the $Mn(L2)_2/\bar{S}i$ complex demonstrates the lowest activity in the reaction: the reaction rate decreases to 0 $\left(C^{f}_{O_3} = C^{in}_{O_3}\right)$ in 50 min. A high activity is demonstrated by the $Mn(L3)_2/\bar{S}i$ complex: the reaction rate decreases from 3.6×10^{-7} to 2.5×10^{-7} mol/(g·s) in 100 min; in other words, the ozone concentration at the reactor outlet decreases only by 50 mg/m^3.

Manganese(II) complexes with L1, L4, L5, and L6 ligands occupy an intermediate position. A trend of ozone decomposition by manganese(II) complexes to occur in a steady-state mode can be seen in Fig. 2a. It is especially apparent for complexes containing L4 and L6 ligands. The duration of the stationary portion for $Mn(L4)_2/\bar{S}i$ exceeds 600 min. During the reaction with ozone, the Mn(II) complexes, except for inactive $Mn(L2)_2/\bar{S}i$, became brown or brownish black (Table 1). Such a color change indicates that Mn(II) turns into Mn(IV) in its oxide form which is a secondary catalyst of ozone decomposition less active than Mn(II) complexes: the reaction rate of ozone decomposition in the steady-state mode is low.

As an example, Fig. 3 demonstrates how the reaction rate for ozone decomposition by $Mn(L1)_2/\bar{S}i$ changes with increasing the initial ozone concentration in OAM from 2.1×10^{-6} to 8.4×10^{-6} mol/l (100–400 mg/m^3). It is obvious that the initial reaction rate (W_{in}) measured after

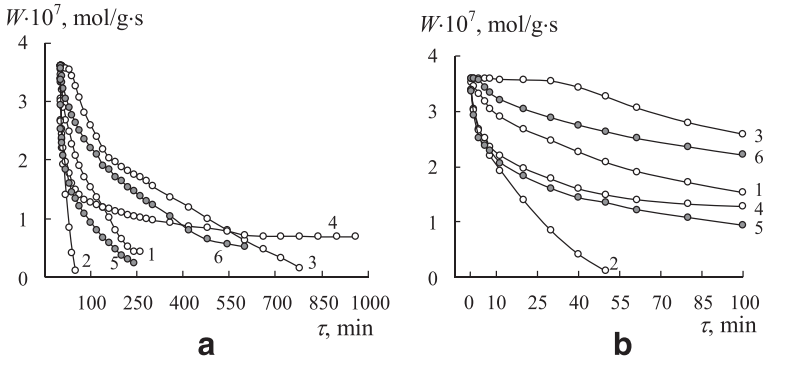

Fig. 2 The time dependences of W for ozone decomposition by $Mn(L)_2/\bar{S}i$ complexes (L = L1–L6): $Mn(L1)_2$ (*1*); $Mn(L2)_2$ (*2*); $Mn(L3)_2$ (*3*); $Mn(L4)_2$ (*4*); $Mn(L5)_2$ (*5*); $Mn(L6)_2$ (*6*) **a** for 1000 min and **b** for first 100 min $\left(C^{in}_{O_3} = 4.2 \times 10^{-6}\text{mol/l}\right)$

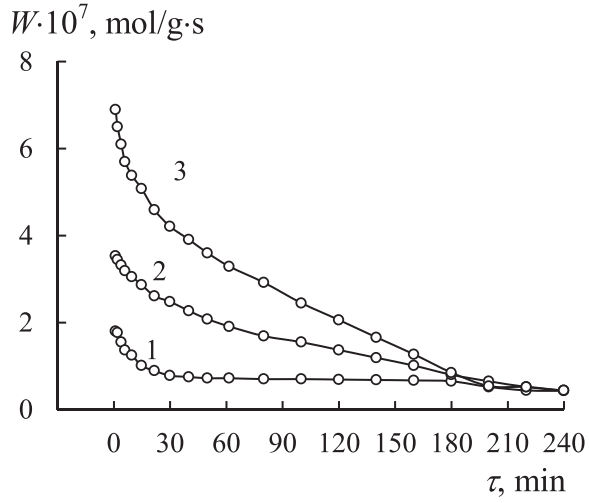

Fig. 3 The time dependences of W for ozone decomposition by $Mn(L1)_2/\bar{S}i$ at $C^{in}_{O_3} \times 10^6$, mol/l: 2.1 (*1*); 4.2 (*2*); 8.4 (*3*) ($C_{Mn(II)} = 6.0 \times 10^{-5}$ mol/g)

1 min of OAM passing increases in proportion to $C^{in}_{O_3}$. It is evidence of the first-order reaction with respect to ozone.

Kinetic and Stoichiometric Parameters of the Reaction of Ozone Decomposition by $L/\bar{S}i$ and $Mn(L)_2/\bar{S}i$ Nanocompositions

To analyze the data obtained, kinetic (W, k_1, $\tau_{1/2}$, $k_{1/2}$) and stoichiometric (Q_{exp}, Q_{CH}, n_L, n_{CH}, n_{Mn}) parameters of the reaction were considered. Their values in the case of $C^{in}_{O_3}$ varying in the presence of $Mn(L1)_2/\bar{S}i$ are summarized in Table 3. As can be seen, all stoichiometric parameters in the series increase with the rise in $C^{in}_{O_3}$. The first-order reaction rate constant, k_1, is invariant only at the beginning of the reaction. Then, it decreases, varies within the series, and is not equal to the reaction rate constant, $k_{1/2}$, corresponding to the time of half-conversion of ozone, $\tau_{1/2}$. The half-conversion time is shortened with $C^{in}_{O_3}$ increasing. These results allow the assumption that the reaction of ozone decomposition proceeds by the radical chain mechanism. Similar regularities were obtained for other $Mn(L)_2/\bar{S}i$ complexes (L = L2–L6).

Table 4 summarizes the results of the kinetic study of ozone decomposition by immobilization on nanosilica Schiff bases (Fig. 1) and their Mn(II) complexes (Fig. 2) at $C^{in}_{O_3} = 4.2 \times 10^{-6}$mol/l. It can be seen that the immobilized Schiff bases can independently decompose ozone. The values of their kinetic constant k_1 calculated for the first 10–20 min of the runs depend on the ligand nature and change in the order L5 < L2 < L3 < L1 < L6 < L4. To the moment of ozone half-conversion, $k_1 \neq k_{1/2}$. The stoichiometric coefficient, n_L, is less than 1 for L1–L3 ligands and exceeds 1 for L4–L6 ligands. Coefficient n_{CH} characterizing completeness of oxidation of the hydrocarbon part of the ligands does not exceed 30 %, i.e., the complete decomposition of the ligands does not occur in one cycle.

The values of k_1 are similar for the free ligands and for their complexes with manganese(II). It can be caused by the fact that, at the beginning of the reaction, an ozone molecule interacts with the same reaction site, i.e., a C=N group. $k_{1/2}$ values do not coincide with k_1 ones indicating a change in the reaction order with respect to ozone due to occurring side chain-radical reactions.

Stoichiometric coefficients n_L increase for the manganese(II) complexes as compared with the corresponding ligands; the fact that $n_{Mn} >> 1$ (the maximum value is observed for $Mn(L3)_2/\bar{S}i$) suggests a multiple participation of Mn(II) in the reaction of ozone decomposition and a catalytic behavior of the complexes.

A catalytic effect of manganese appears also in the increase of n_{CH} coefficient. The values of n_{CH} exceeding 100 % can be due to additional ozone decomposition by manganese in its oxide form.

Judging from the results of kinetic investigations of ozone decomposition by $Mn(L)_2/\bar{S}i$ complexes, the nature of the ligands considerably affects the kinetic and stoichiometric parameters of the reaction. Since the nanocompositions obtained as a result of the synthesis differ in their manganese(II) content, it can be concluded that the immobilized Schiff bases differ in their affinity to metal ions. To compare the activity of complexes, the value of k_1 was calculated for 1 mol of the manganese ion. The catalytic activity of isostructural pseudotetrahedral bis-ligand complexes, $Mn(L)_2/\bar{S}i$ (L = L1–L5), determined in such a way, increases in the order $Mn(L3)_2 >> Mn(L4)_2 > Mn(L1)_2 > Mn(L2)_2 > Mn(L5)_2$. The substitution of L4 for L6 changes the geometry of the Mn(II) coordination polyhedron from pseudotetrahedral (Scheme 1) to pseudooctahedral (Scheme 2). This change in the complex structure results in the more

Table 3 Effect of $C^{in}_{O_3}$ on kinetic and stoichiometric parameters of the reaction of ozone decomposition by $Mn(L1)_2/\bar{S}i$ ($C_{Mn(II)} = 0.6 \times 10^{-4}$; $C_L = 7.0 \times 10^{-4}$ mol/g)

$C^{in}_{O_3} \times 10^6$, mol/l	$W_{in} \times 10^7$, mol/(g·s)	$k_1 \times 10^3$, s^{-1}	$\tau_{1/2}$, s	$k_{1/2} \times 10^4$, s^{-1}	$Q_{exp} \times 10^5$, O_3 moles	$Q_{CH} \times 10^5$, O_3 moles	n_L	n_{CH}, %	n_{Mn}
2.1	1.7	3.6	6600	1.0	30.2	74.7	2.2	40.0	25.2
4.2	3.5	3.8	4800	1.4	42.1	74.7	3.0	56.0	38.3
8.4	7.0	3.8	3900	1.8	49.7	74.7	3.6	66.5	41.4

Table 4 Kinetic and stoichiometric parameters of the reaction of ozone decomposition by $Mn(L)_2/\bar{S}i$ complexes ($C^{in}_{O_3} = 4,2 \times 10^{-6}$mol/l)

Sample	$k_1 \times 10^3$, s^{-1}	$\tau_{1/2}$, s	$k_{1/2} \times 10^4$, s^{-1}	$Q_{exp} \times 10^5$, O_3 moles	$Q_{CH} \times 10^5$, O_3 moles	n_L	n_{CH}, %	n_{Mn}
L1	3.8	1800	3.8	11.1	74.7	0.8	15.0	–
Mn(L1)	3.8	4800	1.4	42.1	74.7	3.0	56.0	38.3
L2	2.8	960	7.2	10.6	72.3	0.8	15.0	–
Mn(L2)	2.4	600	11.5	6.4	72.3	0.5	9.0	4.0
L3	3.2	1600	4.3	12.3	116.7	0.9	10.5	–
Mn(L3)	–	13,800	0.5	127.2	116.7	9.1	109.0	374.1
L4	6.2	3300	2.2	26.0	86.4	1.8	30.0	–
Mn(L4)	6.0	1680	4.1	101.0	86.4	7.0	117.0	63.1
L5	1.3	240	28.8	13.2	45.0	1.8	29.0	–
Mn(L5)	1.6	1080	6.4	35.3	45.0	4.7	78.0	15.0
L6	5.6	2820	2.4	19.6	84.0	1.4	23.0	–
Mn(L6)	5.1	10,200	0.7	93.7	84.0	6.7	111.0	66.8

smooth decrease in the reaction rate at the beginning of the reaction for $Mn(L6)_2/\bar{S}i$ than for $Mn(L4)_2/\bar{S}i$ (Fig. 2a, b); the $\tau_{1/2}$ parameter for the first complex is eight times as much as that for the second complex (Table 3), and therefore, the steady-state mode of ozone decomposition is attained sooner for $Mn(L4)_2/\bar{S}i$ (Fig. 2). The mentioned data allow us to conclude that the structure factor has some influence on the kinetics of ozone decomposition and reactivity of the complexes, but its effect is not governing. More likely, a determining factor is the effect of the redox potential of the Mn^{3+}/Mn^{2+} pair on the reaction rate constant of ozone decomposition by the $Mn(L)_2/\bar{S}i$ complexes. Judging from the data obtained for crystalline complexes of manganese(II), this redox potential depends on the nature of ligands and substituents in both the aldehyde [26, 28, 36–39] and imine [40] components of the complexes. Because of some difficulties in the process of measuring redox potentials of nanosilica-immobilized manganese complexes, the influence of electronic effects of substituents on the reaction rate constant at the beginning of the reaction was analyzed using the classic Hammett equation. The catalytic activity of $Mn(L)_2/\bar{S}i$ complexes decreases in the order of ligands L4 > L1 > L2 > L5, and that agrees with the increase in electron-acceptor properties of substituents in their benzene rings. In conformity with the Hammett equation, a linear dependence with the negative ρ value (–0.61) has been obtained. Such a dependence demonstrates the increase in the electron density on the central atom and the decrease in the reactivity of the complexes towards a strong oxidizer, namely, ozone.

Conclusions

The investigations have shown that the oxidation state of manganese(II) does not change upon the synthesis of its complexes with nanosilica-immobilized Schiff bases. L1–L5 ligands form the complexes with the same pseudotetrahedral coordination polyhedron, N_2O_2. The L6 ligand, because of its steric factors, forms the pseudooctahedral polyhedron, N_2Y_4 (Y—other ligands, namely, H_2O, Cl^-), and its bond with the central atom is realized only through nitrogen of imine group.

Nanocomposites represented by the immobilized Schiff bases, $L/\bar{S}i$, and manganese(II) complexes, $Mn(L)_2/\bar{S}i$, demonstrated their activity in the reaction of low-temperature ozone decomposition. The reactivity of the nanosilica-immobilized Schiff bases increases in the order L5 < L2 < L3 < L1 < L6 < L4. Manganese(II), as a part of the complexes, shows its catalytic properties in the reaction of ozone decomposition. In the case of the isostructural $Mn(L)_2/\bar{S}i$ complexes (L = L1–L5), the number of catalytic cycles (n_{Mn}) increases in the order $Mn(L3)_2 >> Mn(L4)_2 > Mn(L1)_2 > Mn(L2)_2 > Mn(L5)_2$. The change in the geometry of a coordination polyhedron in the case of L4 and L6 does not considerably affect the kinetic and stoichiometric parameters of the reaction. The effect of a substituent in the initial aldehyde component of Schiff bases on the reaction rate constant in the case of ozone interaction with the complexes consisting of manganese(II) and L1, L2, L4, and L5 ligands can be described by the Hammett equation with ρ = –0.61.

Competing Interests
The authors declare that they have no competing interests.

Authors' contributions
OG and ER performed the synthesis and identification of the nanocomposites consisting of manganese(II) complexes with immobilized Schiff bases. AT studied the ozone decomposition kinetics. TR developed the methodology of

the analysis of reaction kinetic and stoichiometric parameters and generalized the obtained results. All authors read and approved the final manuscript.

Authors' information

TR worked as a Head of the Department of Inorganic Chemistry and Chemical Ecology of the Odesa I.I. Mechnikov National University. Her research interests are nanochemistry, nanotechnology, coordination chemistry, and catalysis of redox reactions. AT worked as a docent of the Department of Inorganic Chemistry and Chemical Ecology of the Odesa I.I. Mechnikov National University. Her research interests are nanochemistry, coordination chemistry, and catalysis of the ozone decomposition reaction. ER worked as an engineer of the Department of Inorganic Chemistry of the Taras Shevchenko National University of Kyiv. His research interests are nanomaterials and coordination compounds. OG works as a professor at the Department of Inorganic Chemistry of the Taras Shevchenko National University of Kyiv and as the Dean of the Faculty of Natural Sciences of the National University of Kyiv-Mohyla Academy. His research interests are nanochemistry, nanobiotechnology, and coordination chemistry.

Acknowledgements

The study was carried out with the support of the Ministry of Education and Science of Ukraine.

Author details

[1]Odesa I.I. Mechnikov National University, 2 Dvoryanska str., Odesa 65082, Ukraine. [2]Taras Shevchenko National University of Kyiv, 64 Volodymyrska str., Kyiv 01601, Ukraine. [3]National University of Kyiv-Mohyla Academy, 2 Skovorody str., Kyiv 04655, Ukraine.

Received: 26 October 2015 Accepted: 26 November 2015
Published online: 08 December 2015

References

1. McGarrigle EM, Gilheany DG (2005) Chromium- and manganese-salen promoted epoxidation of alkenes. Chem Rev 105(5):1563–1602
2. Weiss R, Riley D (1999) Therapeutic aspects of manganese(II)-based superoxide dismutase mimics; in uses of inorganic chemistry in medicine. In: Furrell N (ed). The Royal Society of Chemistry, Cambridge, pp 77–99
3. Vos DE, Sels BF, Jacobs PA (2001) Immobilization of homogeneous oxidation catalysts. Adv Catal 46:1–87
4. Padmanabhan M, Varghese A (1999) Structural modification of copper(II) complexes with the use of polymer supports. Oriental J of Chemistry 15(1): 79–84
5. Suja NR, Yusuff KKM (2004) Cobalt(II), nickel(II), and copper(II) complexes of polystyrene-supported Schiff bases. J Appl Polymer Sci 91(6):3710–3719
6. Gupta KC, Abdulkadir HK, Chand S (2004) Synthesis, characterization and catalytic activity of N, N′-bis(3-allyl salicylidene)ethylenediamine cobalt(II) Schiff base complex anchored on a new polymer support. Chinese J Polymer Sci 22(1):31–42
7. Gupta KC, Abdulkadir HK, Chand S (2003) Polymer-immobilized N,N ′-bis(acetylacetone)-ethylendiamine cobalt(II) Schiff base complex and its catalytic activity in comparison with that of its homogenized analogue. J Appl Polymer Sci 90(5):1398–1411
8. Santwana G, Beena S (2003) Synthesis of a polystyrene anchored Schiff base and its complexes with some 3d-transition metals. J Ind Chem Soc 80(9): 841–842
9. Hu DD, Shi QZ, Tang ZX, Fang Y, Kennedy JF (2001) CoSalen immobilized to chitosan and its electrochemical behavior. Carbohydr Polym 45(4):385–393
10. Chang Y, Wang Y, Zha F, Wang R (2004) Preparation and catalytic properties of chitosan bound Schiff base complexes. Polym Advan Technol 15(5):284–286
11. Silva AR, Vital J, Figueiredo JL, Freire C, Castro B (2003) Activated carbons with immobilised manganese(III) salen complexes as heterogeneous catalysts in the epoxidation of olefins: influence of support and ligand functionalisation on selectivity and reusability. New J Chem 27(10):1511–1517
12. Silva AR, Martins M, Freitas MMA, Valente A, Freire C, Castro B et al (2002) Immobilisation of amine-functionalised nickel(II) Schiff base complexes onto activated carbon treated with thionyl chloride. Micropor Mesopor Materials 55(3):275–284
13. Silva AR, Freire C, Castro B, Freitas MMA, Valente A, Figueiredo JL (2001) Anchoring of a nickel(II) Schiff base complex onto activated carbon mediated by cyanuric chloride. Micropor Mesopor Materials 46(2–3):211–221
14. Silva AR, Freitas MMA, Freire C, Castro B, Figueiredo JL (2002) Heterogenization of a functionalized copper(II) Schiff base complex by direct immobilization onto an oxidized activated carbon. Langmuir 18(21):8017–8024
15. Murphy EF, Ferri D, Baiker A (2003) Novel routes to Cu(salicylaldimine) covalently bound to silica: combined pulse EPR and situ attenuated total reflection-IR studies of the immobilization. Inorg Chem 42(8):2559–2571
16. Chisem IC, Rafelt J, Shieh MT, Chisem J, Clark JH, Jachuck R et al (1998) Catalytic oxidation of alkyl aromatics using a novel silica supported Schiff base complex. Chem Commun 18:1949–1950
17. Feng HX, Wang RM, He YF, Lei ZQ, Wang YP, Xia CG et al (2000) Preparation and catalysis of porous silica supported metal Schiff-base complex. J Molec Catalysis A: Chemical 159:25–29
18. Murphy EF, Schmid L, Burgi T, Maciejewski M, Baiker A, Gunther D et al (2001) Nondestructive sol-gel immobilization of metal(salen) catalysts in silica aerogels and xerogels. Chem Mater 13(4):1296–1304
19. De Vos DE, Dams M, Sels BF, Jacobs PA (2002) Ordered mesoporous and microporous molecular sieves functionalized with transition metal complexes as catalysts for selective organic transformations. Chem Rev 102(8):3615–3640
20. Saha PK, Banerjee S, Saha S, Mukherjee AK, Sivasanker S, Koner S (2004) Immobilization of a metal complex in Y-zeolite matrix: synthesis, X-ray single-crystal, and catalytic activities of a copper (Schiff-base)-Y zeolite based hybrid catalyst. Bull Chem Soc Jpn 77(4):709–714
21. Deshpande S, Srinivas D, Ratnasamy P (1999) EPR and catalytic investigation of Cu(salen) complexes encapsulated in zeolites. J Catalysis 188(2):261–269
22. Koner S (1998) Novel color isomerism and catalytic activities of Cu(salen) complex encapsulated in a zeolitic matrix. Chem Commun 5:593–594
23. Poltowicz J, Pamin K, Tabor E, Haber J, Adamski A, Sojka Z (2006) Metallosalen complexes immobilized in zeolite NaX as catalysts of aerobic oxidation of cyclooctane. Appl Catal Gen 299:235–242
24. Kim GJ, Shin JH (1999) The synthesis of new chiral salen complexes immobilized on MCM-41 by grafting and their catalytic activity in the asymmetric borohydride reduction of ketones. Catal Letters 63:205–212
25. Rakitskaya TL, Truba AS, Raskola LA, Radchenko EA, Strizhak AV, Golub AA (2013) Antiozonant activity of the silica modified with 3d metal complexes. Rus J Gen Chem 83(2):360–367
26. Bhadbhade MM, Srinivas D (1993) Effects on molecular association, chelate conformation, and reactivity toward substitution in copper Cu(5-X-salen) complexes, salen^{2-} = N,N′-ethylenebis(salicylidenaminato), X = H, CH3O, and Cl: synthesis, X-ray structures, and EPR investigations. Inorg Chem 32(26): 6122–6130
27. Tas E, Aslanoglu M, Guler M, Ulusoy M (2004) Synthesis, characterization and electrochemical properties of copper(II) complexes with novel bidentate salicylaldimines derived from 3,5-DI-t-butyl-2-hydroxybenzaldehyde. J Coord Chem 57(7):583–589
28. Chellamani A, Kulanthaipandi S, Rajagopal S (1999) Oxidation of aryl methyl sulfoxides by oxo(salen)manganese(V) complexes and the reactivity-selectivity principle. J Org Chem 64(7):2232–2239
29. Rakitskaya TL, Truba AS, Raskola LA, Bandurko AY, Golub AA (2006) Effect of the structure of copper(II) complexes adsorbed on the surface of SiO_2 on their catalytic activity in ozone decomposition. Theoret Experim Chem 42(1):60–66
30. Rakitskaya TL, Truba AS, Golub AA, Kiose TA, Radchenko EA (2011) Effect of composition and structure of cobalt(II) complexes with oxyaldiminopropylaerosils on their catalytic activity in the decomposition of ozone. Theor Experim Chem 47(5):337–341
31. Tertyh VA, Chuiko AA, Khrenovskii VA, Neimark IE (1968) Investigation of adsorption properties of amino organic silica by IR spectroscopy. Zh Fiz Khim 42(7):1758–1761
32. Yatsimirskii KB, Chuiko AA, Filippov AP (1977) Copper, molybdenum, and palladium complexes with nitrogen-containing ligands anchored on a silica surface. The Proceedings of the USSR Academy of Sciences 237(5):1137–1139
33. Domenech A, Formentin P, Garcia H, Sabater MJ (2000) Combined electrochemical and EPR studies of manganese Schiff base complexes encapsulated within the cavities of zeolite Y. Eur J Inorg Chem 2000(6):1339–1344
34. Kureshy RI, Ahmad I, Khan NH, Abdi SHR, Pathsk K, Jasra RV (2006) Chiral Mn(III) salen complexes covalently bonded on modified MCM-41 and SBA-15 as efficient catalysts for enantioselective epoxidation of nonfunctionalized alkenes. J Catal 238(1):134–141
35. Silva AR, Wilson K, Clark JH, Freire C (2006) Covalent attachment of chiral manganese(III) salen complexes onto functionalised hexagonal mesoporous silica and application to the asymmetric epoxidation of alkenes. Micropor Mesopor Materials 91(1–3):128–138

36. Boggess RK, Heghes W, Coleman WM, Taylor LT (1980) Preparation and electrochemical studies of tetradentate manganese(III) Schiff base complexes. Inorg Chem Acta 38(2):183–189
37. Venkataramanan NS, Premsingh S, Rajagopal S, Pitchumani K (2003) Electronic and steric effects on the oxygenation of organic sulfides and sulfoxides with oxo(salen)chromium(V) complexes. J Org Chem 68(19): 7460–7470
38. Palucki M, Finney NS, Pospisil PJ, Güler ML, Ishida T, Jacobsen EN (1998) The mechanistic basis for electronic effects on enantioselectivity in the (salen)Mn(III)-catalyzed epoxidation reaction. J Am Chem Soc 120(5):948–954
39. Yildirim LT, Emregul KC, Kurtaran R, Atakol O (2002) Structure and electrochemical behaviour of bis[N-(4-methylphenyl)salicylaldimine]copper(II) N,N′dimethylformamide solvate. Cryst Res Technol 37(12):1344–1351
40. Samide MJ, Peters DG (1998) Electrochemical reduction of copper(II) salen at carbon cathodes in dimethylformamide. J Electroanal Chem 443(1):95–102